RESEARCH ARTICLE

Recombinant Expression and Purification of F-box and Leucine-rich Repeat Protein 5 (FBXL5) using a Prokaryotic Expression System

Fatima Joy C. Cruz[1]*, Tomohide Saio[2], Takeshi Uchida[2], Koichiro Ishimori[2]

*Corresponding author's email address: fccruz2@up.edu.ph

[1]*Department of Physical Sciences and Mathematics, College of Arts and Sciences, University of the Philippines Manila, Manila, Philippines*
[2]*Structural Chemistry Laboratory, Graduate School of Chemical Sciences and Engineering, Hokkaido University, Sapporo, Japan*

ABSTRACT

Background: The F-box and Leucine-rich Repeat Protein 5 (FBXL5), a member of the E3 ligases, is considered to be the central iron sensor in mammals. The cryo-EM structure of FBXL5 in complex with IRP2 and SKP1 was reported by Wang *et al.* in 2020. Surprisingly, a 2Fe-2S cluster seemed to be responsible for the iron-sensing capability of FBXL5.

Methodology: To further explore the mechanism of its regulation, it is important to study the interaction of FBXL5 with other proteins under regulated conditions so we attempted to express FBXL5 in the hopes of studying its interaction with IRPs *in vitro*.

Results: Plasmids were constructed to express FBXL5 in Escherichia coli expression hosts. Purification of an MBP-fused FBXL5 and a GST-fused FBXL5 were performed using affinity chromatography. Peptide Mass Fingerprinting, Circular Dichroism spectroscopy, and SEC-MALS were employed to analyze the purified MBP-FBXL5. GST-FBXL5 was also used in a pull-down assay with Iron Regulatory Protein 1 (IRP1).

Results: We are successful in expressing and partially purifying full-length FBXL5 using E. coli with the aid of a protein tag, the maltose binding protein (MBP) tag. However, cleavage of the protein tag resulted in decreased stability of FBXL5 as shown in SEC-MALS data. CD spectroscopy showed consistent secondary structure of FBXL5. A preliminary pull-down assay of GST-FBXL5 with IRP1 showed that IRP1 displayed interaction with the recombinant GST-FBXL5.

Conclusion: FBXL5, a 78-kDa mammalian protein was overexpressed in a prokaryotic expression system made stable by a fusion protein. The interaction of GST-FBXL5 with IRP1 also shows that it is possible to study their interaction *in vitro*.

Keywords: *FBXL5, iron metabolism, ubiquitin ligase, IRP1*

Introduction

The human body contains an average of three to five grams of iron [1,2]. The liver is the primary storage site of iron where cellular ferritin acts as a reservoir. The rest of the iron is distributed in the bone marrow and muscles while macrophages recycle iron from dead red blood cells. Every day, the body loses around one to two milligrams of iron through the sloughing of epithelial cells and iron lost must be replenished through the diet.

Iron is important to promote the growth of cells and allow biochemical reactions to proceed but iron can also generate reactive oxygen species (ROS) especially when iron is in excess. ROS can cause damage to cells by reacting with cellular membranes, DNA, and other proteins causing injury to the liver and other organs [3-5]. In healthy cells, iron is properly regulated otherwise imbalances can lead to diseases. Iron deficiency leads to anemia while iron overload disorders such as hemochromatosis are well reported in literature [6]. Although not clearly established, severe diseases such as cancer, diabetes, and neurodegenerative diseases are related to iron overload conditions.

The adjustment of iron level inside the cell involves an interplay of many factors. Due to its inherent toxicity, free

iron is sequestered by transferrin as it circulates in the body [7]. It binds to Transferrin Receptor 1 (TfR1) and enters the cell through endocytosis [8]. Through acidification by a proton pump, the iron is released from the transferrin inside the vesicle and transported out to the cytoplasm through a metal transporter [1]. Iron becomes part of the hypothetical cytosolic labile iron pool (LIP) and is transported to different parts of the cell where it is needed. For example, it is transported to the mitochondria to be incorporated into heme or the excess iron is stored by ferritin (Figure 1)[1,9].

The cell adjusts its level of iron through Iron Regulatory Proteins (IRPs). These are post-transcriptional molecules that regulate iron levels by binding to Iron Responsive Elements (IREs) found on the 5' or the 3' end of mRNAs coding for ferritin – the iron storage protein – and transferrin receptor 1 (TfR1) – an iron uptake receptor [1,4,9-11]. Bound IRP on the 5' end of ferritin mRNA blocks the ribosome thus preventing its translation while that on the 3' end of TfR1 mRNA blocks the binding of endonuclease thus allowing translation [12]. The increase in expression of TfR1 allows more iron to enter the cell. On the other hand, when there is a high amount of iron, IRPs dissociate from IREs and the opposite effect takes place, ferritin is expressed while TfR1 mRNA is degraded by the endonuclease. These processes are shown in Figure 2.

In 2009, two groups separately discovered a new pathway in the regulation of the mRNA-binding activity of IRPs. This involved the F-box and leucine-rich repeat protein 5 (FBXL5), a 78-kDa protein [13,14]. FBXL5 can interact with IRPs leading to their ubiquitination and degradation by the proteasome. This interaction was promoted in excess iron concentrations but not observed in the presence of an iron chelator. The importance of the FBXL5-IRPs interaction was made clear when deletion of FBXL5 gene in mice resulted in early death in embryos [15].

FBXL5 is part of a complex, the Skp1-Cul-Rbx-F-boxFBXL5, composed of four subunits [13,14]. FBXL5 is a member of the family of F-box proteins which interact with substrates and bring them in proximity to the E2 ubiquitin conjugating enzyme for ubiquitination [16-19]. The complex
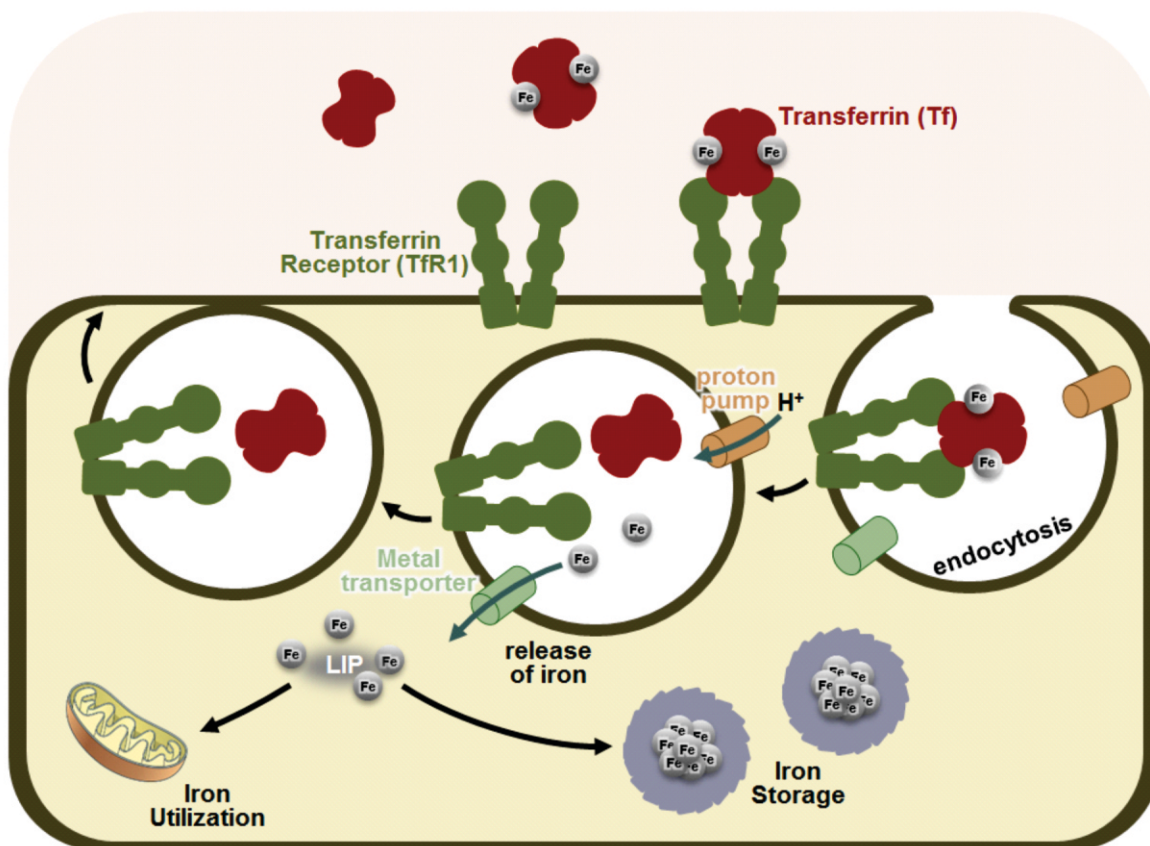

Figure 1. *Iron uptake, utilization and storage inside the cell. Iron bound transferrin enters the cell through interaction with the transferrin receptor TfR1. The iron released temporarily becomes part of the labile iron pool (LIP). Depending on the level of iron inside the cell, iron becomes transported to several areas for utilization or for storage by ferritin.*
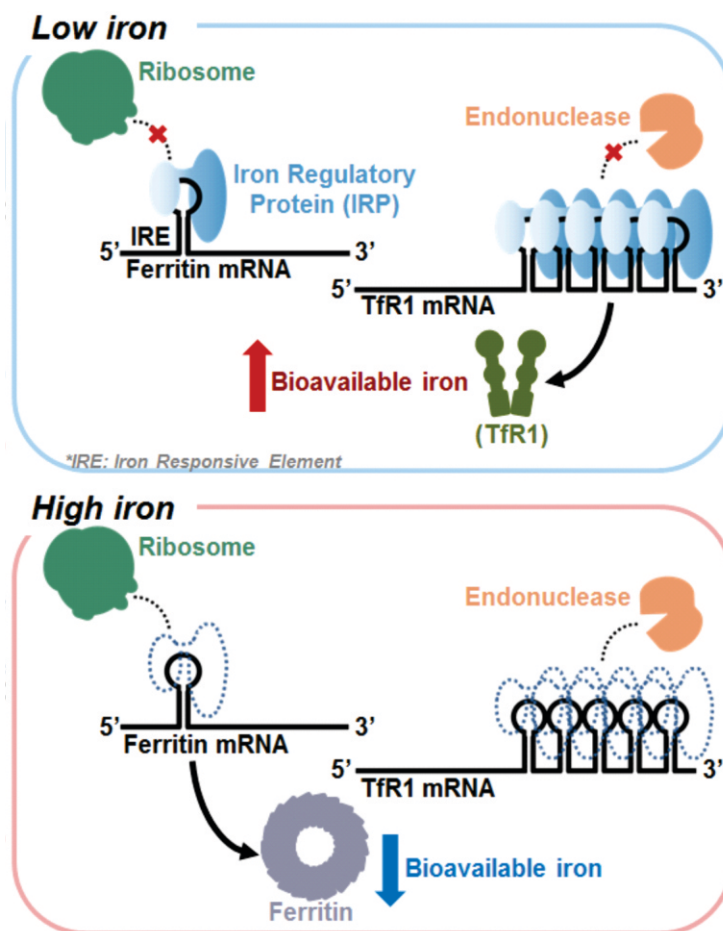
Figure 2. *RNA-binding activity of IRPs. The RNA-binding activity of IRPs depends on the level of iron. At low iron condition, IRPs are bound to mRNA while IRPs are dissociated from mRNAs at high iron levels. When IRPs are bound, the expression of TfR1 is promoted. When dissociated, the expression of ferritin is promoted.*

provides a scaffold allowing the E2 enzyme to attach ubiquitin to the substrate, as shown in the structure of another complex bearing a different F-box protein, Skp2.

All 69 F-box proteins are reported to contain two important structural elements, the F-box domain and the leucine-rich repeats (LRRs) [20]. The F-box domain interacts with the Skp subunit of the E3 ligase complex while the leucine-rich repeats interact with the substrate. However, in the case of FBXL5, an additional domain is in its N-terminal [19]. The hemerythrin-like (Hr-like) domain assumes an elongated structure composed of 5 α helices (Figure 3A) [21,22]. Structural characterization of this domain revealed that it can bind two iron atoms through several glutamate and histidine residues (Figure 3B).

It has been proposed that the iron-binding regulates the stability of FBXL5. By studying the mean molar residual ellipticity at 222 nm with respect to temperature, the melting temperature of the Hr-like domain without bound iron atoms (apo-Hr-like) was lower than that of the Hr-like domain with bound iron atoms (holo-Hr-like) [23]. Studies of N-terminal truncation constructs have shown that several residues considered to be a degron might be responsible for the degradation of FBXL5 [22]. In low iron conditions, FBXL5 cannot bind two iron atoms leading to some structural instability exposing the degron and leading to the degradation of FBXL5. On the other hand, by the binding of iron, FBXL5 is stable and the degron remains buried preventing degradation.

The binding of iron atoms to FBXL5 and its effect to the availability of FBXL5 in cells is linked to its activity as the interaction partner of IRP. As shown in Figure 4, in high iron condition, FBXL5 is more stable and protected from degradation. FBXL5 is available to bind IRP causing the degradation of IRP resulting in increase of ferritin levels and iron storage to decrease the amount of iron available for usage. On the other hand, in low iron condition, the
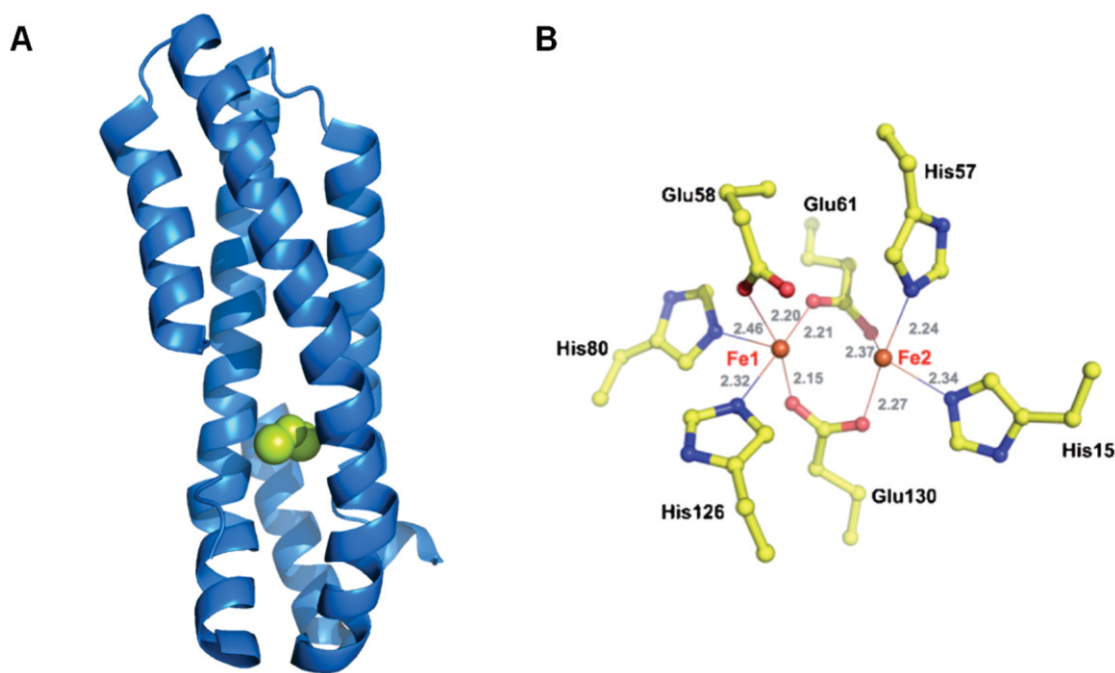
Figure 3. *The hemerythrin-like domain of FBXL5. A) Structure of hemerythrin-like domain showing the two iron as yellow spheres. B) The coordination sphere around the two iron atoms in the hemerythrin-like domain of FBXL5.*
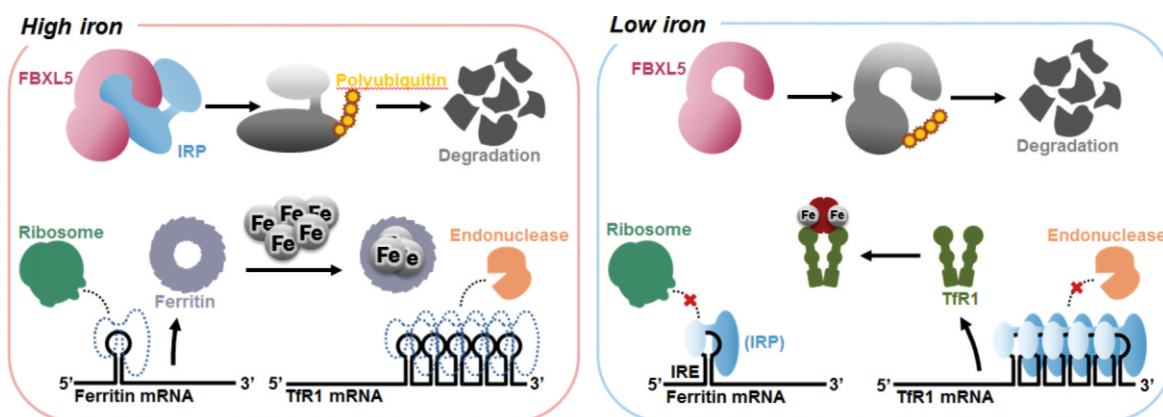

Figure 4. *The effect of FBXL5 on the IRE-binding activity of IRPs in high and low iron conditions. FBXL5 regulates the level of iron in cells by promoting the degradation of IRPs in high iron condition or undergoing degradation in low iron condition.*

proposed degron within the Hr-like domain of FBXL5 is exposed causing its degradation. The decrease in available FBXL5 allows IRPs to bind to IREs and TfR1 is produced leading to an increase in iron uptake.

The molecular mechanism that regulates the FBXL5-IRPs interaction is not yet clear. One hindrance is the difficulty in the recombinant expression of FBXL5. In 2020, a group from University of Washington and New York University School of

Medicine reported the cryo-EM structure of FBXL5 in complex with IRP2 and SKP. They report the presence of a 2Fe-2S cluster in FBXL5 which could be responsible for the iron-sensing capability of the protein [24]. This is a big leap in the study of FBXL5. In order to further explore the function of FBXL5, it is important to study it and its interaction with its partner proteins in a regulated environment. In this study, we attempted to produce the full-length FBXL5 using the E. coli expression system in the hopes of obtaining a high

concentration sample for subsequent structural studies and other in vitro assays. We also attempted to perform in vitro interaction study of FBXL5 with IRP2.

Methodology

Preparation of Plasmids

The pMalc2-His-Pres-FBXL5 plasmid was a kind gift from Assistant Professor Yukiko Takeda of the Graduate School of Medicine, Kyoto University. The FBXL5 cDNA (2076 bp) was inserted using BamHI and XBaI cleavage sites into the pMalc2-His-Pres plasmid (6667 bp) resulting to a vector with a size of 8743 bp. The vector contained the nucleotide sequence for cytoplasmic expression of MBP followed by a hexa-histidine tag, the recognition site for the PreScission Protease and the sequence of full-length FBXL5. Using this plasmid as the template, the FBXL5 nucletoide sequence was amplified by PCR through the Primestar DNA polymerase by Takara Bio, Inc. To express FBXL5 with GST in its N-terminal, pColdGST (5097 bp) was used. Primers for insertion into pColdGST were 5'-GGGCCCGGGACATATGGCGCCCTTTCCTGAAG AAG-3' for sense through the NdeI restriction enzyme and 5'- GCTTGAATT CGGATCCTCATTCGCCAGAGCGGCAG-3' through the BamHI restriction enzyme. One recognition site for NdeI existed within the FBXL5 cDNA sequence at position 977. This was silently mutated using the Primestar Mutagenesis Kit by Takara Bio, Inc. Despite low ligation success rate with NdeI as reported by the manufacturer, it was still chosen as one of the ligation sites because it is closest to the GST tag gene sequence in the vector which reduces the length of the linker from the tag to the FBXL5. To eliminate the template pMalc2 vector, DpnI restriction enzyme was added to the PCR reaction mixture after the run and incubated for 1 to 2 hours. DpnI recognizes the sequence GmA↓TC and cuts between A and T, where mA is a methylated adenine which does not exist in PCR generated nucleotides. The PCR product was purified using a commercial spin column from Qiagen. Digestion with NdeI and BamHI of pColdGST and amplified FBXL5 was performed at 37ºC for 1 hour. Ligation was done at 15ºC for 25 minutes. After ligation, the plasmids were transformed into E. coli DH5α cells and spread on LB agar plate containing ampicillin and incubated overnight at 37ºC. After confirming growth, several colonies were inoculated separately into 5-mL LB medium and cultured overnight at 37ºC. The E. coli cells were harvested and the plasmids were purified using the FastGene® Plasmid minikit from Nippon Genetics Co., Ltd. Confirmation of successful ligation was done through one or more of the following: PCR amplification of the FBXL5 insert or restriction enzyme cleavage followed by agarose gel electrophoresis and sequence analysis.

Expression and Purification of Recombinant FBXL5

FBXL5 was expressed using the pMalc2 vector. FBXL5 was fused to a Maltose-Binding Protein (MBP) tag in the former's N-terminal followed by a hexa-histidine linker. Two liter-culture of transfected Rosetta(DE3) pLysS cells was used and induction was done with IPTG at a final concentration of 1 mM at 15°C overnight. Cells were collected and sonicated for 30-second stages interspersed with 30-second rests for a total of 5 minutes. The lysate was collected and centrifuged at 20000 rpm for 20 minutes and the clear supernatant was obtained.

Affinity chromatography using a pre-packed dextrin sepharose column and the AKTAprime system was used for purification of the MBP-His-FBXL5 construct. The binding buffer used was 50 mM Tris of pH 8.0 with 1 M NaCl and 1 mM EDTA and elution was done with the addition of 10 mM maltose. Fractions containing MBP-His-FBXL5 were collected and 1 mL GST-fused PreScission Protease with an activity of 3 µg mL-1 was added. The sample was incubated overnight in an end-over-end shaker at 4ºC. GST resin was added to the sample, incubated for 30 minutes and centrifuged at 500xg for 5 min. The supernatant was applied to a HiLoad 16/600 Superdex 200 pg column with a running buffer of 50 mM Tris, pH 8.0, and 150 mM NaCl.

Confirmation of Amino Acid Sequence and Molar Mass

Samples of MBP-FBXL5 from SDS-PAGE were cut and de-stained with 50% acetonitrile and 25 mM sodium bicarbonate (NaHCO3). Samples were treated with reducing agent (10 mM DTT) and alkylating agent (1% iodoacetamide) followed by digestion with trypsin. Peptides from the gel were extracted with 0.1% trifluoroacetatic acid and 50% acetonitrile. Peptide samples were prepared using C18 Ziptip (EMD Millipore Corp.) and loaded onto the plate with CHCA matrix. After drying, the plate was loaded into a Bruker Corp. AutoflexTM speed MALDI-TOF machine. Ten scans were performed for each sample and the average spectrum was obtained. Each spectrum was post-processed with the BioTools software of FlexAnalysisTM.

For the SEC-MALS analysis, around 200 µL of each sample was pipetted into the sample vial and the sample vial was loaded into the sample injector. A buffer of 50 mM Tris and 150 mM NaCl at pH 8.0 was used for the SEC-MALS analysis. The temperature was set to 4ºC and the sample was loaded onto a Superdex 75 10/300 GL column. The eluate directly flowed to a cell where it is hit by a laser with a wavelength of 658 nm. Data collection was performed at one second
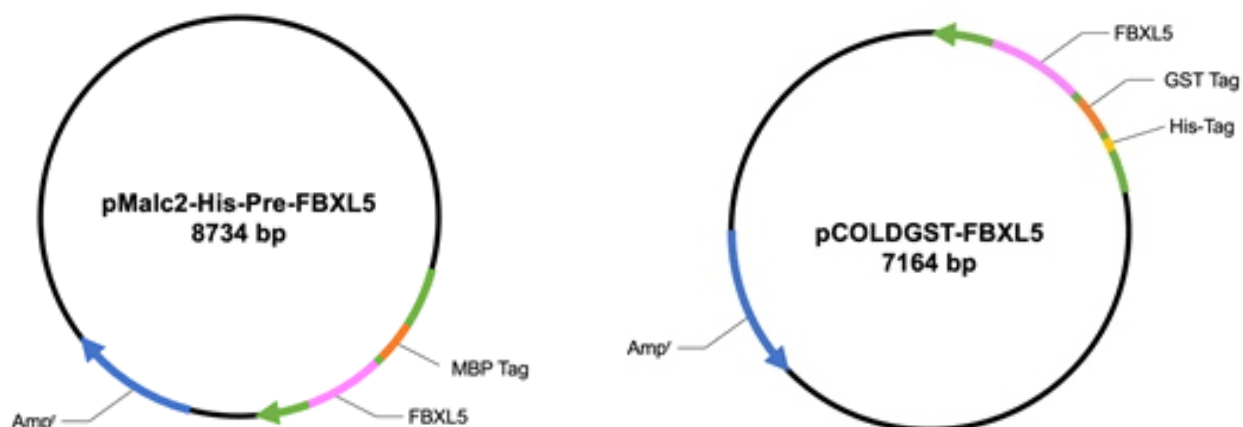
Figure 5. *Plasmid constructs used in expressing FBXL5. The plasmids pMalc2-His-Pres-FBXL5 (left) and pCOLDGST-FBXL5 (right) were used in the prokaryotic expression of FBXL5. The latter was constructed using the former as the template for the FBXL5 gene sequence.*

intervals. Intensity of scattered light were measured at a total of 8 angles. Analysis was performed with the ASTRA5 software that incorporates a number of analytical tools one of which is molar mass determination via light scattering.

Secondary Structure Analysis

Around 600 to 700 µL of sample in 50 mM Tris and 150 mM NaCl, pH 8.0 was used for circular dichroism spectroscopic analysis. MBP-His-FBXL5 had a concentration of around 7 µM while FBXL5 had a concentration of around 5 µM. Measurement was done three times from 250 to 200 nm with a scan rate of 20 nm/minute.

Pull-down Assay

The pColdGST-FBXL5 plasmid was used to express FBXL5. One liter of Rosetta (DE3) pLysS culture was induced overnight at 15ºC with IPTG at a final concentration of 1 mM. Cells were collected and lysed with 50 mM Tris buffer, pH 8.0 with 500 mM NaCl and 0.1% NP-40. Immobilized metal affinity chromatography with Ni-NTA resin was used to capture the His6-GST-FBXL5 from the cell lysate. Washing was done with 50 mM Tris buffer, pH 7.4. IRP1 was expressed using the baculovirus-High Five insect cell expression system. Purification was done according to a previous protocol established in our laboratory.[25] Purified IRP1 was incubated with the captured FBXL5 for 1.5 hours. Washing was done with 50 mM Tris, pH 7.4. Elution was performed with 200 mM imidazole. SDS-PAGE analysis was performed to confirm the proteins present in the washings and eluate.

Results

Plasmid Constructions

The insertion of FBXL5 cDNA into the pColdGST plasmid (Figure 5) was confirmed through PCR amplification of the FBXL5 insert or restriction enzyme cleavage followed by agarose gel electrophoresis and sequence analysis. Several colonies were selected from an ampicillin plate and seperately cultured. Plasmids from these colonies were purified and the FBXL5 sequence was amplified and checked using agarose gel electrophoresis. Colonies that showed bands corresponding to the size of the FBXL5 cDNA (2067 bp) were confirmed as those bearing the vectors that were successfully ligated.

Restriction enzyme digestion with NdeI and BamHI were also performed on the vectors purified from selected colonies. After incubation with the restriction enzyme digest, the samples were analyzed using agarose gel electrophoresis alongside with the intact sample (not treated with restriction enzymes). Samples that showed two bands for the size of the plasmid (5097 bp) and the FBXL5 cDNA (2067 bp) were confirmed for successful ligation. Additional confirmation was also performed by sequencing analysis following the protocol of PCR kit used. The results showed that using the NdeI site for the insertion of the FBXL5 gene sequence was successful as well. No issues must be encountered in the silent mutation performed on the NdeI site within the FBXL5 gene sequence because the mutation was silent. Samples that were confirmed to contain the FBXL5 cDNA were stored at -20°C until further use.
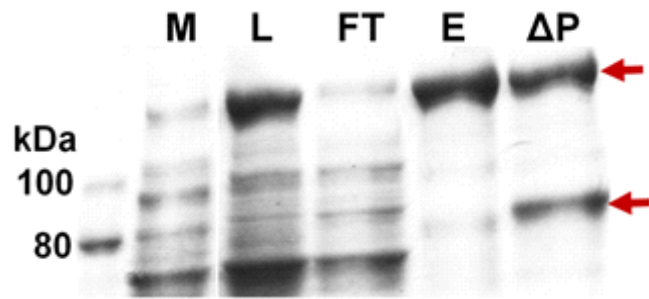
Figure 6. *Result of purification of MBP-His-FBXL5. Buffer containing 1 M NaCl was used. (M: Molecular mass marker, L: Cell lysate, FT: Column flowthrough, E: Column eluate, ΔP: After 1 hour incubation with protease)*
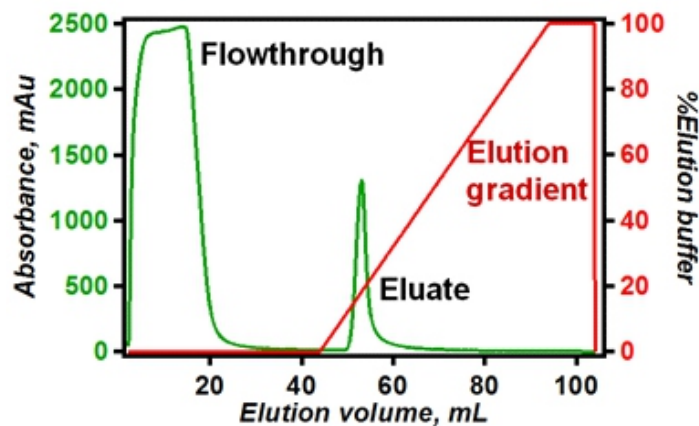

Figure 7. *Affinity chromatography of cell lysate. Elution profile of 20-mL cell lysate loaded onto 5-mL MBPTrap showing the flowthrough and eluate.*

Figure 8. *Intensity profile of the cell lysate SDS-PAGE lane generated with GelAnalyzer2010a. The band and peak for MBP-His-FBXL5 is indicated with a red arrow.*

Figure 9. *Intensity profile of the MBPTrap eluate SDS-PAGE lane generated with GelAnalyzer2010a. The band and peak for MBP-His-FBXL5 is indicated with a red arrow.*

Purification of MBP-His-FBXL5

Purification of MBP-His-FBXL5 was done with 5-mL MBPTrap by GE Healthcare Life Sciences© based on the affinity of the MBP with the maltose polymer supported on the resin. Initially, the buffer contained NaCl with a concentration of 200 mM. However, analysis with SDS-PAGE revealed that MBP-His-FBXL5 co-eluted with relatively high amount of unwanted proteins. This result indicate that there are non-specific interactions between the resin and other proteins in the cell lysate. There may also be non-specific interactions between MBP-His-FBXL5 and unwanted proteins. The concentration of the salt was not enough to prevent these non-specific interactions, and it was increased to 500 mM but the results were not improved. When 1 M NaCl was used in the buffer, the result greatly improved. The SDS-PAGE shown in Figure 6 showed a clear band for MBP-His-FBXL5 with very minimum bands for unwanted proteins. The chromatogrom shown in Figure 7 clearly showed the high efficiency of the affinity column as MBP-His-FBXL5 eluted as a single peak.
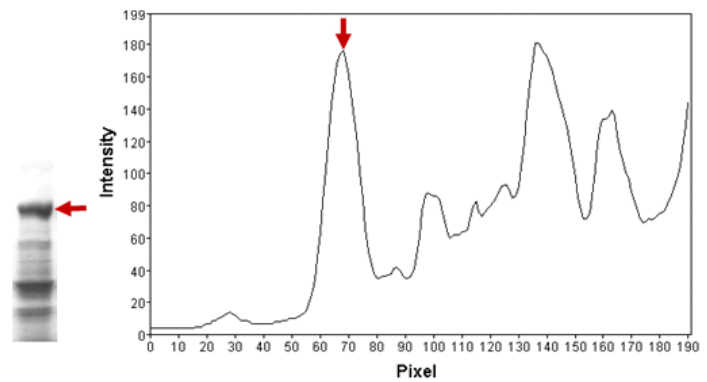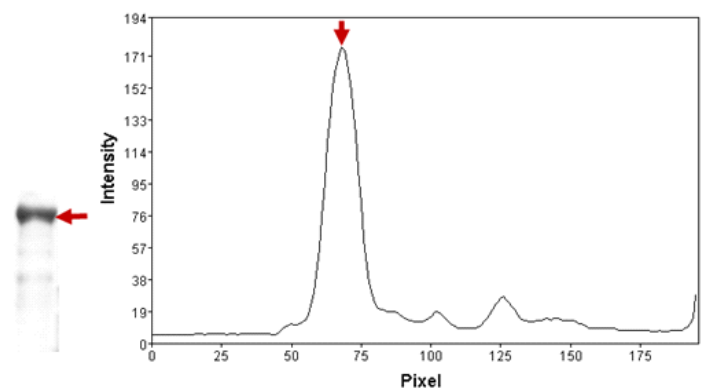
Using GelAnalyzer2010a the intensity profiles of lanes L and E in Figure 6 were obtained. The lane for the lysate (L) with its corresponding intensity profile is show in Figure 8. The red arrow indicates the band for MBP-His-FBXL5 with its corresponding peak on the profile. Taking the peak area for MBP-His-FBXL5 and getting its ratio against the total peak areas, the amount of MBP-His-FBXL5 in the cell lysate was estimated to be around 27%.

The intensity profile for the eluate (E) lane is shown in Figure 9. Based on the peak volume, MBP-His-FBXL5 comprised around 82% of the eluate. Comparing the peak volumes of MBP-His-FBXL5 in the cell lysate and in the eluate, the yield of the affinity chromatography is more than 90%. The concentration of the eluate was measured using the theoretical molar extinction coefficient of MBP-His-FBXL5 as reported by the ExPasy ProtParam Tool by the Swiss Institute of Bioinformatics (URL: http://web.expasy.org/protparam/) [26].

The MBP tag was cleaved from FBXL5 using the PreScission Protease enzyme which recognizes the sequence

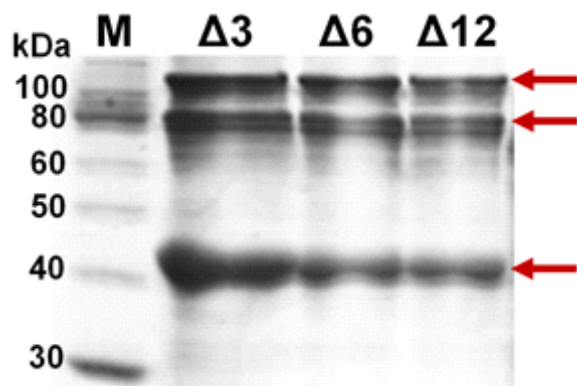**Figure 10.** *Time course analysis of PreScission protease activity. Samples were taken after 3 (Δ3), 6 (Δ6) and 12 (Δ12) hours of incubation at 4ºC.*

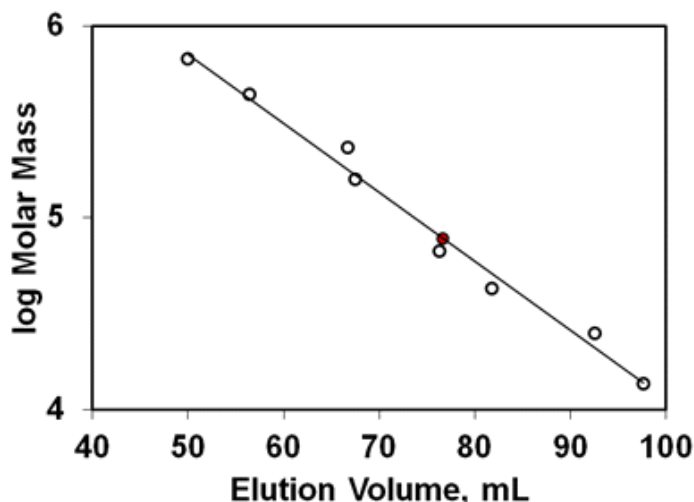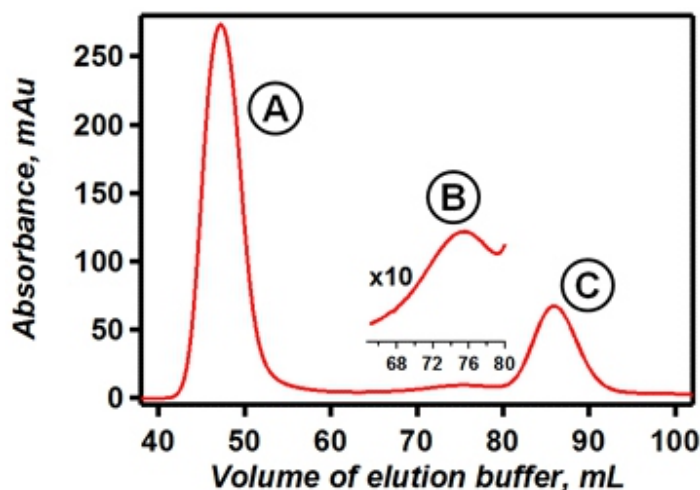**Figure 11.** *Elution profile of 15 mL sample collected after affinity chromatography loaded onto a gel filtration column. The profile shows three peaks marked A, B, and C. Peak A corresponds to the void volume, peak B to FBXL5 and peak C to MBP.*
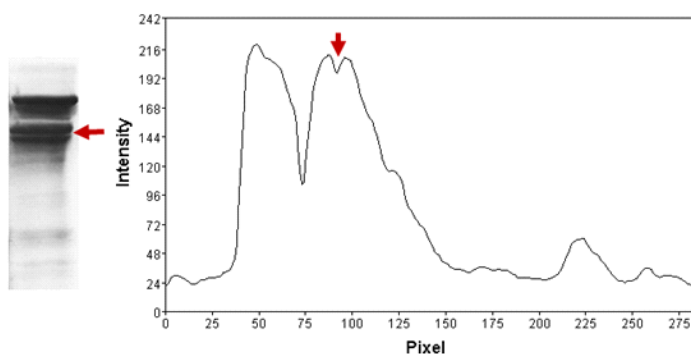

Figure 12. *Confirmation with SDS-PAGE of fractions obtained from gel filtration chromatography.*

Figure 13. *Reference curve for HiLoad 16/600 Superdex 200pg. The red dot corresponds to the elution volume of peak B in Figure 22.*

Figure 14. *Intensity profile of the SDS-PAGE lane for the peak B fraction from gel filtration generated with GelAnalyzer2010a. The band and peak for FBXL5 is indicated with a red arrow.*
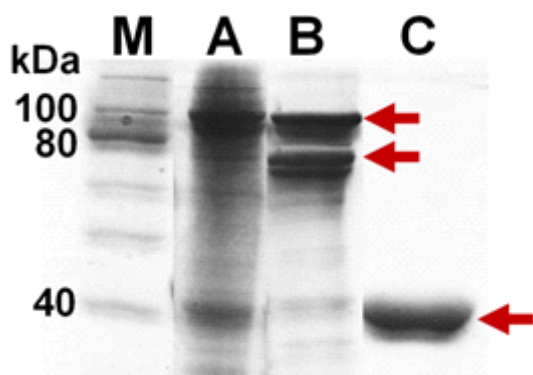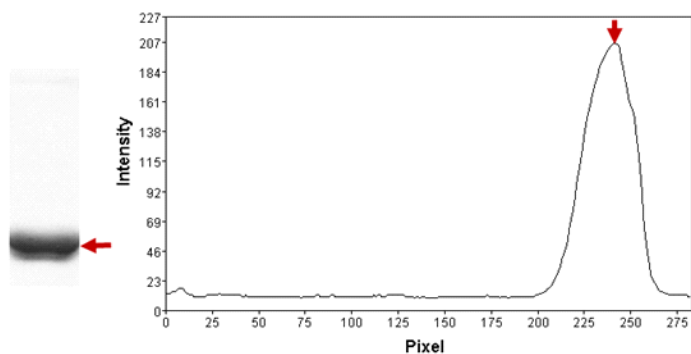

Figure 15. *Intensity profile of the SDS-PAGE lane for the peak C fraction from gel filtration generated with GelAnalyzer2010a. The band and peak for MBP is indicated with a red arrow.*

Leu·Glu·Val·Leu·Phe·Gln↓Gly·Pro and cuts between Gln and Gly as shown by the arrow in the sequence. Incubation at 4ºC after 1, 3, 6 and 12 hr samples were analyzed with SDS-PAGE. After 1 hour, 50% of the protein was cleaved as show in lane ΔP of Figure 6. After that, the efficiency of the cleavage did not change as shown in Figure 10.

To separate FBXL5 from uncleaved MBP-His-FBXL5 and MBP, gel filtration chromatography was performed using a buffer with NaCl concentration of 150 mM. The profile is shown in Figure 11. Three peaks can be observed, one at the void volume (A), another at elution volume around 75 mL (B) and the third peak at elution volume around 86 mL (C). Each fraction corresponding to the three peaks was collected and analyzed with SDS-PAGE shown in Figure 12. The void volume (Figure 11, peak A) fraction showed many bands (Figure 12, lane A), a sign of instability and degradation of MBP-His-FBXL5. The band for uncleaved MBP-His-FBXL5 was also present. Its elution at the void volume meant that it was misfolded and aggregated with each other. Peak B of the elution profile is at a volume corresponding to the molecular mass of FBXL5 (78 kDa) based on the reference curve in Figure 13 as shown by the red shaded dot. As shown by the

two bands in the SDS-PAGE MBP-His-FBXL5 co-eluted with free FBXL5. The free MBP was recovered in the pure state as shown by lane C of Figure 12. Using the GelAnalyzer2010a, the intensity profiles of the lanes for B and C of Figure 12 were obtained. The intensity profiles are shown in Figures 14 and 15. The peak volumes for FBXL5 and MBP were compared. The peak volume for FBXL5 was around 8000 units while the peak volume for MBP was around 7000 units. The almost equal peak volume values of the two proteins indicated almost equal amount of proteins obtained in the gel filtration chromatography. This meant that there was no spontaneous cleavage of MBP from FBXL5 and that cleavage by the protease was successful.

Confirmation of Recombinant Expression

In recombinant protein expression, tracking of the recombinant protein is always done with SDS-PAGE. However, this is not confirmatory as it is possible that other proteins are present in the same band. Other proteins in the cell lysate can have the same molecular mass as the recombinant protein. The identity of the protein giving the suspected band on an SDS-PAGE gel was confirmed by peptide mass fingerprinting.
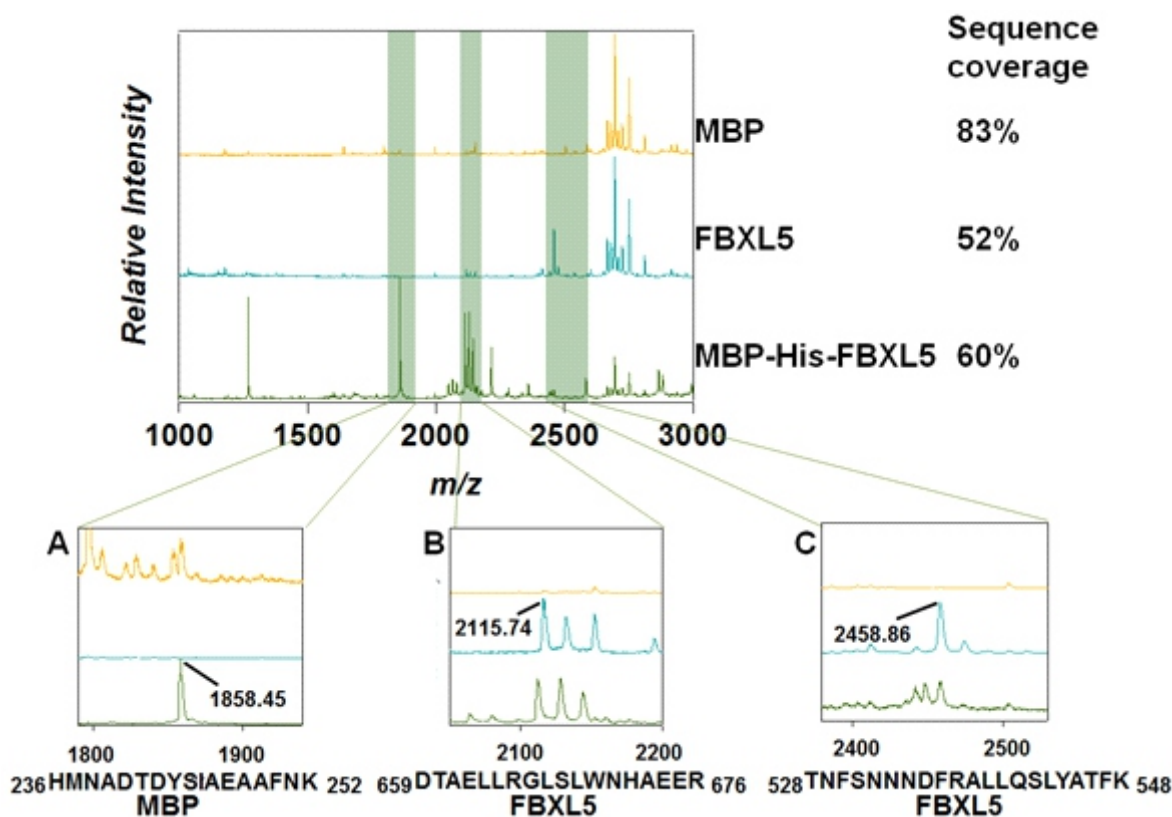

Figure 16. *MALDI-TOF mass spectra of MBP, FBXL5 and MBP-His-FBXL5. CHCA matrix was used in reflector mode; some peaks are enlarged and shown with their corresponding peptide.*
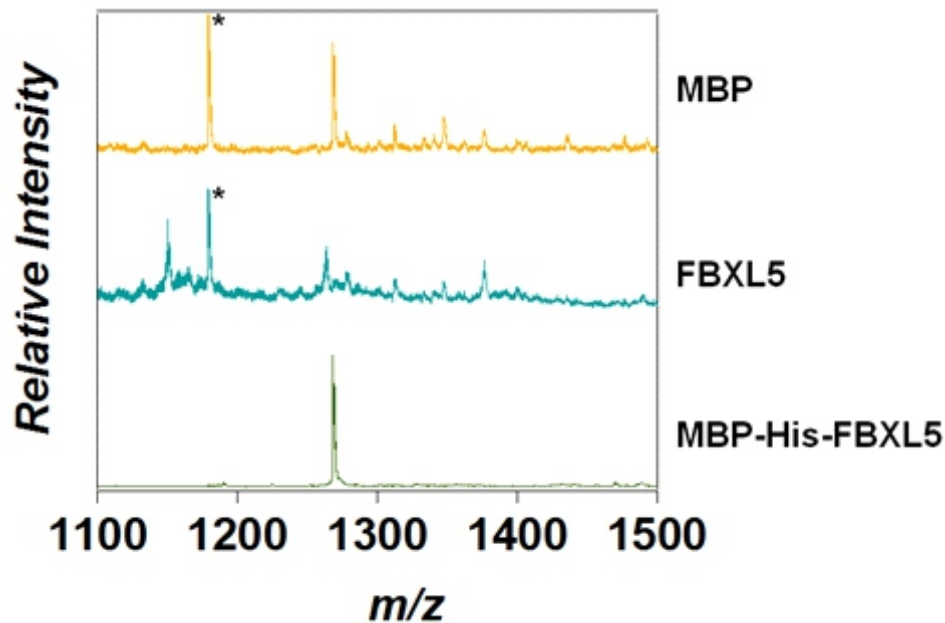
Figure 17. *Peak due to tryptic digestion of keratin. Peak at m/z=~1180 Da marked by asterisks on the spectra of MBP and MBP-His-FBXL5*
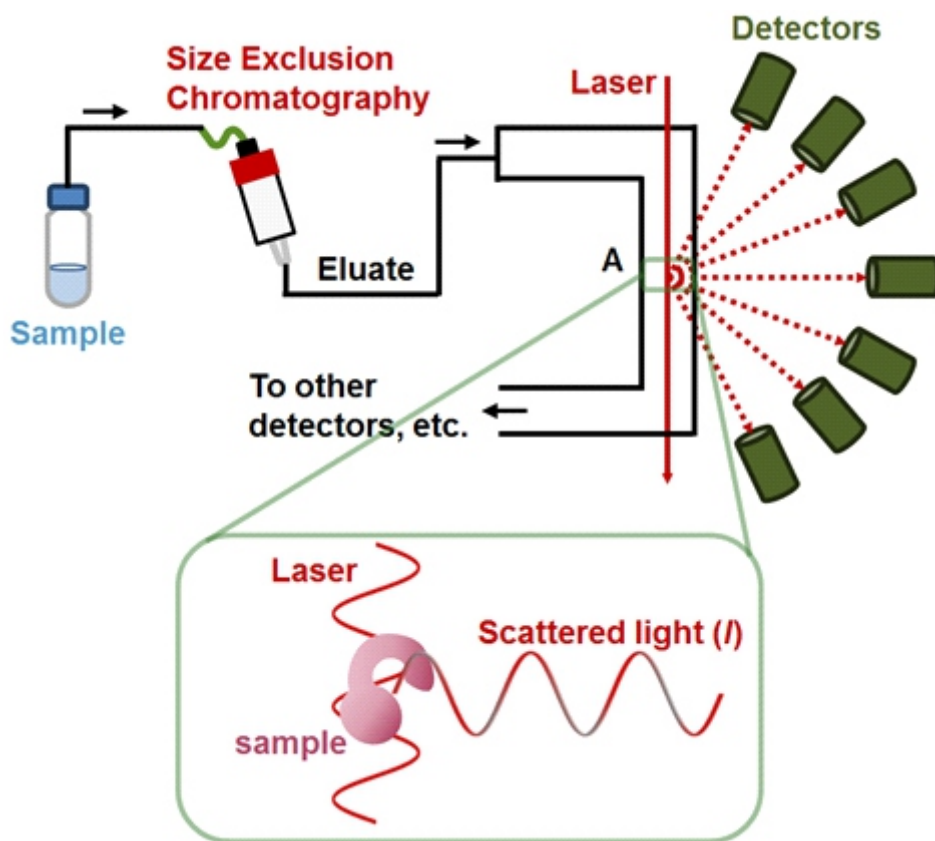

Figure 18. *SEC-MALS Principle. A schematic diagram showing the relationship of the components of the SEC-MALS and the sample.*

Peptide Mass Fingerprinting

Peptide mass fingerprinting (PMF), or peptide mass mapping, is one conventional method of protein identification [27]. Bands from the SDS-PAGE corresponding to MBP-His-FBXL5, FBXL5 and MBP were used as samples for PMF. Theoretically, the combined spectra of MBP and FBXL5 should be the same as the spectrum of MBP-His-FBXL5. A quick glance of the three spectra on Figure 16 reveals that it was not the case. One reason is that there are different peptides generated from the three samples that have the same molar mass and thus will be observed as a peak with the same m/z value in the three spectra. Contamination of sample with keratin during preparation would also lead to peptides generated from tryptic digestion of keratin. For example, a peak at around 1180 appeared in the spectra for MBP and FBXL5 (Figure 18). Tryptic digestion of keratin leads to a peptide with a molecular mass of 1179.66 Da.[28] Meanwhile, tryptic digestion of MBP-His-FBXL5 and FBXL5 theoretically generates a peptide with a molecular mass of 1179.38 Da. This peak should appear in the spectra of FBXL5 and MBP-His-FBXL5. But the peak appeared in the spectra for MBP and FBXL5 and not for MBP-His-FBXL5 as shown in Figure 18. Manual inspection of peaks revealed that there are peaks in the MBP spectrum that are also found in the MBP-His-FBXL5 spectrum but not in the FBXL5 spectrum. There were also peaks found in the spectrum of FBXL5 that were in the spectrum of MBP-His-FBXL5 but not MBP. Such peaks are shown in Figure 16. Figure 16A shows a peak with m/z=1858.45 detected in both the spectra for MBP

and MBP-His-FBXL5. Inspection of the list of theoretical peptides of MBP generated by the built-in analysis tool with the Bruker Corp. AutoflexTM speed MALDI-TOF software showed that this peak corresponded to the peptide from MBP with sequence [236]HMNADTDYSIAEAAFNK[252]. Inspection of the theoretical peptide list of MBP-His-FBXL5 also showed the same peptide and no other peptide fragmented from FBXL5 having the same molecular mass was present. On the other hand, Figure 16B and 16C show peaks due to peptides fragmented from FBXL5 and thus were absent in the spectrum of MBP. Despite the contamination from keratin, peaks were manually inspected and some were authentic peptide fragments from MBP, FBXL5 or MBP-His-FBXL5.

To determine the accuracy of each spectrum, the list of theoretical peptides were compared with the list of peaks detected for each spectrum after post-processing. Commonly, an error or deviation from the theoretical is set. This error will determine whether an experimental peak is the same as the theoretical peak. The most commonly used error in peptide mass fingerprinting is 50 ppm. However, when this value was used, no peaks from the spectrum matched with the list of theoretical peptides. In order to increase the number of matched peaks the error was increased to 5000 ppm. For the three samples, an average of 50 peaks were identified. The total amino acid for all peptides corresponding to the identified peaks were counted and their percentage against the total amino acid number of each sample was calculated. For MBP, the corresponding peptides for identified peaks
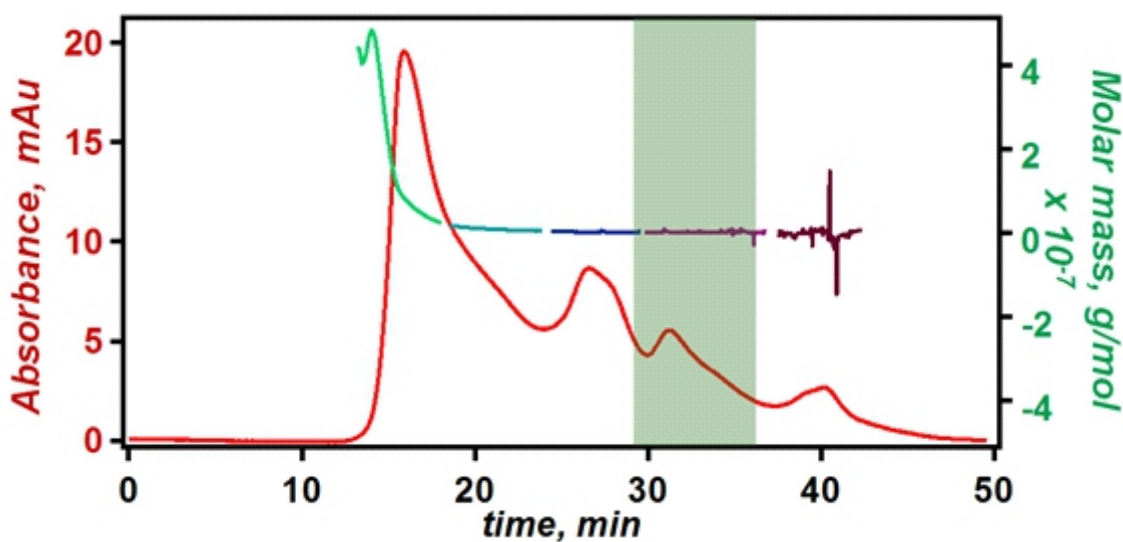

Figure 19. *SEC-MALS data. Spectrum of sample B (from Figures 22 and 23) showing the absorbance of the eluate through time with the corresponding molar mass obtained with DAWN8+, Wyatt Technology.*
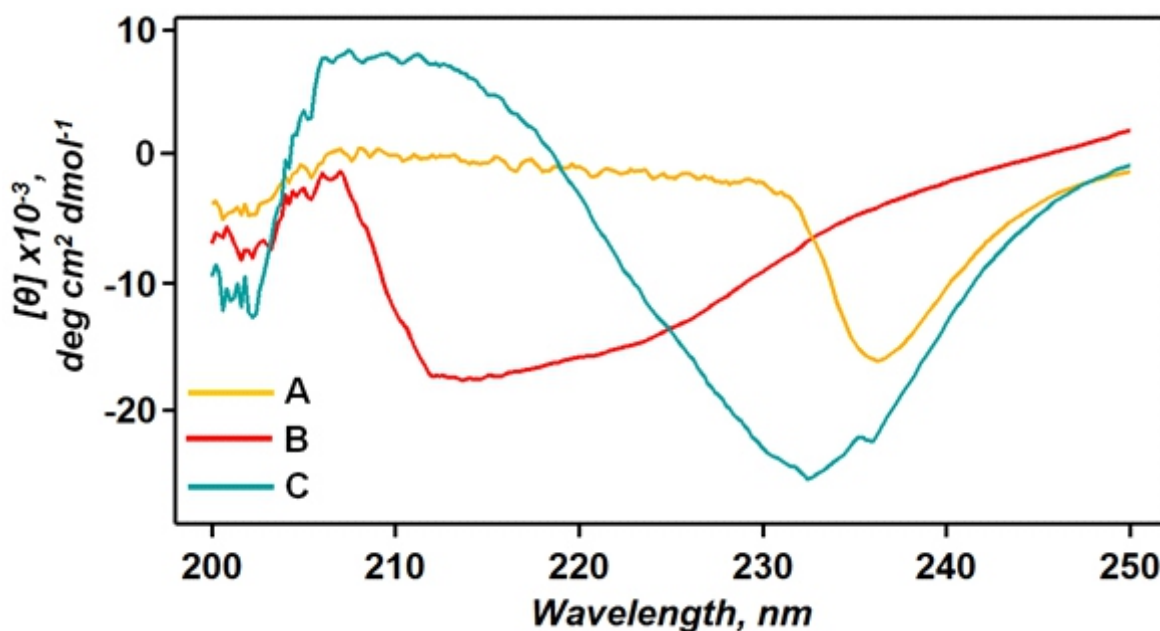
Figure 20. *Secondary structural analysis. CD spectra of three fractions collected from gel filtration chromatography measured in 50 mM Tris buffer, pH 8.0 with 150 mM NaCl.*

cover 83% of its total amino acid sequence. For FBXL5 and MBP-His-FBXL5, the sequence coverage values were 52% and 60% respectively. MBP, FBXL5 and MBP-His-FBXL5 were identified using peptide mass fingerprinting.

SEC-MALS

Size Exclusion Chromatography-Multiangle Light Scattering is a technique that determines the molar mass of a pure sample. The fraction corresponding to peak B in Figure 11 was collected and run into the size exclusion column before analysis with multiangle light scattering. Each eluate reaching the cell (Figure 18, point A) gets hit by a laser. The particles in the sample scatter the light and the intensity of the scattered light (I) is measured by detectors positioned at several angles. I is directly proportional to the molar mass of the sample.

The obtained SEC-MALS is shown in Figure 19. The absorbance of each eluate that passes through the cell in time is shown in the left y-axis. The corresponding molar mass of the eluate is shown as a scatter plot with reference to the right y axis. Using the ASTRA5 software interface, peaks were manually set. The software then calculated the average molar mass for each peak set. The output showed that the third peak shaded green in Figure 19 had an average molar mass of 72580 g/mol or Da which is comparable to the molar mass of FBXL5, 78000 Da. The average molecular masses for the other peaks are showin in Table 1. All other eluates had

very high molecular masses. Peak 1 corresponded to an aggregate while peaks 2 and 4 correponded to a supposed FBXL5 dimer and trimer, respectively. Whether FBXL5 forms such multimers is yet to be confirmed.

Secondary Structural Analysis

After confirmation of the molecular mass of FBXL5 with SEC-MALS, the proper folding of FBXL5 was confirmed through the analysis of secondary structure using CD spectroscopy. Fractions A, B and C from the gel filtration chromatogram (Figure 11) were analyzed. Figure 20 shows the three CD spectra of samples A, B and C. It is interesting to observe that the CD spectrum of peak B had a profile distinct for an α helical protein. While that of sample A had a peak at around 230 nm showing loss of secondary structure.[30] These two samples were observed to contain both MBP-His-FBXL5 and FBXL5 based on SDS-PAGE and yet they displayed

Table 1. *Average molecular masses for peaks on SEC-MALS profile*

Peak	Average molecular mass (g/mol or Da)
1	6 707 000
2	155 900
3	72 580
4	205 700
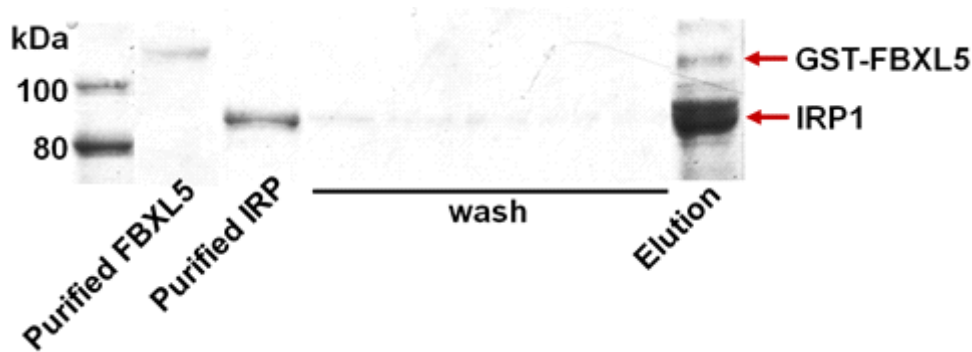
Figure 21. *Result of pull-down assay. SDS-PAGE of purified FBXL5 and IRP with the wash and elution samples.*
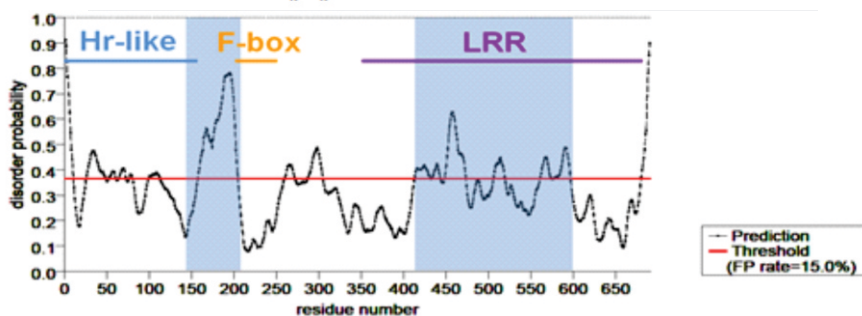

Figure 22. *Amino acid sequence of FBXL5 and result of prediction. Upper) The amino acid sequence of FBXL5 showing in color code the different domains: Hr-like, F-box, LRR. Lower) Result of PrDOS showing predicted disordered regions in FBXL5*

different secondary structural properties. For sample C which is expected to be pure MBP, a protein with 40% of amino acids in α helix, the obtained CD spectrum showed no characteristic peaks at 208 and 222 nm. The three samples from the gel filtration chromatography had observable differences in their secondary structures.

The α helical content of the protein can be calculated based on its ellipticity at 222 nm [30]. Using the following equation, the α helical content of sample B was determined. $[\theta]222$ refers to the ellipticity at 222 nm and fH is the fraction of α helix.

$$[\theta]_{222} = -30300\, f_H - 2340 \qquad \text{[Eq. 1]}$$

The obtained f_H value for the sample B which contained the pure intact FBXL5 is 0.40 or 40%. For reference, the secondary structure of FBXL5 was predicted using the PredictProtein Server (URL: https://www.predictprotein.org/). The amino acid sequence of FBXL5 was used by the server to predict whether an amino acid within the residue would be most likely found in an α helix, β strand or loop. The results gave a value of 43% meaning that 297 amino acid residues in FBXL5 most likely form α helical structure. The nearness of the similar value obtained from the prediction to that from the CD spectrum indicates that FBXL5 in sample B was in its native conformation.

In vitro Interaction of FBXL5 and IRP1

The recombinant expression system designed above was successful in producing FBXL5 using the MBP tag. However, after cleavage of MBP, FBXL5 becomes highly unstable and lost its secondary structure leading to aggregation. To investigate the interaction of FBXL5 and IRP1 in vitro without requiring the cleavage of the tag, the pull down assay is a very appropriate technique. This small-scale method requires only a low concentration and amount of sample (in the microliter range) thus the low yield previously observed will be useful for the investigation. GST tag was fused to the N-terminal of FBXL5 while it was reported that the LRRs in the C-terminal interact with the substrates of FBXL5 [14]. It is expected that GST will not interefere with the interaction of FBXL5 and IRP1.

After incubation at 4ºC of FBXL5 and IRP1, washings and the eluate were collected. SDS-PAGE was run and the image is show in Figure 21. The two bands on the Elution lane signified the co-elution of FBXL5 and IRP1. The amount of IRP1 that eluted was higher than that of FBXL5 as indicated by the intensity of the bands measured using the GelAnalyzer2010a.

The higher amount of IRP1 that eluted from the resin may refer to non-specific interactions between IRP1 and the resin. It is recommended to perform a reference pull down assay between the GST and IRP1 which was not performed in this study. This reference pull down assay can provide the background interactions taking place without FBXL5. These background interactions can then be subtracted from the pulldown assay between FBXL5 and IRP1 thus providing the actual interaction between FBXL5 and IRP1.

Nevertheless, the result from the pull down assay showed that FBXL5 and IRP1 can interact in vitro. This is an unexpected result because FBXL5 is known to interact with IRPs in high iron concentration. Considering that the assay was performed without any iron added to the sample, it means that IRP1 and FBXL5 are in their apo states. Just like the case of IRP2, FBXL5 might be the E3 ubiquitin ligase that recognizes apo–IRP1 and promotes its proteasomal degradation in high iron conditions [31]. With the recent finding of Wang, et.al., it is possible that the 2Fe-2S cluster discovered in FBXL5 is also responsible for the recognition of IRP1 by FBXL5 as shown by Wang's FBXL5-IRP1 model structure [24].

Discussion

The problem with non-specific interactions by unwanted proteins was solved by increasing the salt concentration to 1 M. The increase in ionic strength did not affect the interaction of MBP with the resin as MBP interacts with the dextrin on the sepharose resin primarily by hydrogen bonding. The use of such high salt concentration in protein purification is not new. A group reporting the crystal structure of a deaminase that restricts the activity of retrovirus replication used 1 M NaCl in its lysis buffer [32]. The use of a high salt concentration in this study improved the yield of recombinant MBP-His-FBXL5.

After the affinity chromatography, it was desired to remove the protein tag as it can hinder the interaction of FBXL5 with IRP during the pull down assay. MBP is a large protein with a molecular mass of 43 kDa. The PreScission Protease was used to cleave MBP-His from FBXL5. Even after overnight incubation at 4ºC, the 50% activity of the protease did not change. This might be due to the high concentration of salt in the buffer. The high salt concentration prevented the necessary interaction between MBP-His-FBXL5 and the protease. At first, buffer exchange was not performed as, in a separate experiment, it was found out that FBXL5 forms aggregates with time even if it was left on ice. If a higher protease activity is desired buffer exchange to one with a lower salt concentration prior to cleavage with the protease is recommended.
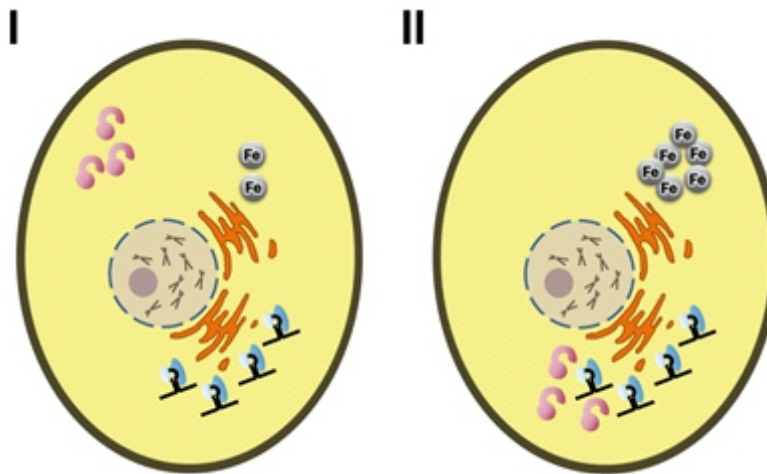
Figure 23. *Proposed cellular event in which FBXL5 becomes co-localized with IRP1 in high iron condition.*

To obtain the purified intact FBXL5 after cleavage of MBP-His, gel filtration chromatography was performed to separate FBXL5 from uncleaved MBP-His-FBXL5 and MBP. In this step, problem arose as several bands were observed in the SDS-PAGE of the fractions collected after gel filtration. After cleavage of MBP, the misfolded FBXL5 aggregated and came out in the void volume. One possibility for this is that after its synthesis, FBXL5 is misfolded and MBP helped it to remain stable. It seemed that MBP is essential for FBXL5 to remain stable.

Based on the gel filtration chromatography results (Figures 12 and 13), the fraction corresponding to the peak equivalent to the molecular weight of FBXL5 contained the MBP-His-FBXL5. Based on the standard curve in Figure 14, MBP-His-FBXL5 should elute at a lower volume. Probably, this MBP-His-FBXL5 was misfolded and assumed a linear conformation thereby increasing its retention time in the resin. This fraction was subsequently analysed with SEC-MALS. The size exclusion result should have two peaks as observed by the two bands on the SDS-PAGE in Figure 12, lane B. The experimental profile gave four peaks as shown in Figure 20. The other peaks corresponded to aggregated forms as given by the average molecular masses as presented in Table 1. Thus, as time passes during the purification stage, FBXL5 loses its native structure and aggregates. Changes in environmental factors such as temperature contribute to the structural change in FBXL5. Highly unstable proteins such as FBXL5 need a purification protocol that requires less time but highly efficient.

In addition to this, an online prediction tool called Protein Disorder Prediction System (PrDOS, URL: http://prdos.hgc.jp/cgi-bin/top.cgi)[33] was used to look at the possibility of disordered regions in FBXL5. The prediction involved an algorithm that scans the amino acid sequence and calculates the probability that a certain amino acid flanked by its neighbors is found in a disordered region. This algorithm is also based on empirical data such as known structural information of other protens. The results are shown in the lower portion of Figure 22. The high peaks in the graph correspond to amino acids that possess high probability to be disordered. Amino acids in the region between the hemerythrin-like domain and the F-box domain and those within the LRRs of FBXL5 are predicted to be disordered. Contrary to stable globular proteins, such disordered regions are recognized to be barriers to recombinant protein expression as they are described to be lacking in proper structure by having highly flexible backbones [33,34].

Despite this, the PMF confirmed the expression of the recombinant protein by identifying the amino acid sequence of FBXL5 from samples extract from the SDS-PAGE gel. The sequence coverage values obtained in the PMF were relatively high but the reliability of these values is low because of the high error set to identify peaks. The difficulty in obtaining high accuracy in PMF studies is due to contamination mainly by human skin and keratin. There are a lot of keratin sources during the experiment. These include hand-made gels and buffers, gel tanks and table surfaces. Use of fresh buffers and clean equipment and frequent changing of gloves are highly advisable to lessen contamination. Subtraction of peaks from such contaminant proteins can also be done. Increasing the concentration of the applied sample can also improve the result by making the relative intensity of contaminant peaks negligible. The molecular mass of FBXL5 was also determined by SEC-MALS. The

resemblance of the CD spectrum of FBXL5 to that of an α helical protein and the comparable experimental and theoretical α helicity values confirmed the proper folding of FBXL5. These results show that the recombinant expression of FBXL5 using *E. coli* was successful.

The interaction of FBXL5 and IRP1, although weak, even in the absence of iron was quite surprising. This weak interaction may be brought about by hydrophobic interactions between the LRRs of FBXL5 and some unidentified region in IRP1. To translate this result to a cellular setting where the interaction is known to be iron-dependent, one possibility is that there is some sort of initial localization (Figure 23 I) followed by translocation of one of either proteins (Figure 23 II). The translocation is brought about by high iron conditions and allows the two proteins to co-localize and interact leading to the proteasomal degradation of IRP1. This reflects how the cell controls processes via localization of proteins. Whenever the state of the cell changes, increase or decrease of iron concentration for example, signal cascades take place which lead to changes in the localization of proteins. Previous reports claim that FBXL5 was shown to localize in the nuclues as it targets a different substrate, the zinc finger transcription factor Snail1 that controls the expression of proteins involved in cellular motility.[35] One possibility is that FBXL5 could be transported from the nucleus to the cytoplasm to target IRPs. Whether this function is linked to FBXL5 targeting Snail1 in the nucleus is yet to be determined.

Conclusions

The predicted disordered regions in FBXL5 could prevent the successful recombinant expression with E. coli. This was successfully resolved with the use of protein tag specifically the MBP tag. The amino acid sequence, molecular mass and secondary structure of the intact FBXL5 was confirmed by PMF, SEC-MALS and CD spectroscopy. However, in the purification stage, the cleavage of the tag led to high instability in FBXL5 causing it to aggregate and lowering the yield.

The interaction of FBXL5 and IRP1 was monitored using the pull down assay in the absence of iron. Surprisingly, both proteins co-eluted from the resin showing weak interaction without iron. This interaction is supposed to be brought by hydrophobic interactions between the LRRs of FBXL5 and some unidentified region in IRP1. Inside the cell, many factors are localized in areas where they can perform their function. In the case of FBXL5, in low or normal iron condition is it found in yet unknown location inside the cell, away from the IRP/IRE system. Otherwise, FBXL5 could readily interact with free IRP1 and cause

its degradation. Then, in high iron condition, FBXL5 changes its location by still unknown process ang reaches the IRP/IRE system where it can interact with IRP1 and cause its degradation.

This study was able to successfully express full-length FBXL5 using *E. coli*. However, due to instability, the yield was low. In order to increase the yield of FBXL5, the baculovirus expression vector system (BEVS) will be used for eukaryotic expression of FBXL5. Eukaryotic expression provides the needed post-translational modifications of eukaryotic proteins which are absent in bacteria. These modifications can also increase the stability of recombinant proteins.

Furthermore, the study has shown, albeit with a certain degree of confidence, that the investigation of the interaction between FBXL5 and IRP1 and IRP2 can be performed using the pull down assay technique. The dependence of the interaction on the amount of iron and heme will be investigated in order to clarify the molecular mechanism that regulates FBXL5-IRP interaction.

References

1. Pantapolous K, Porwal SH, Tartakoff A, Devireddy L. (2012) Mechanisms of Mammalian Iron Homeostasis. Biochemistry 51(29):5705-5724.
2. Hentze MW, Muckenthaler MU, Andrews NC. (2004) Balancing acts: Molecular Control of Mammalian Iron Metabolism. Cell 117(3):285-297.
3. Bystrom LM, Guzman ML, Rivella S. (2014) Iron and Reactive Oxygen Species: Friends or Foes of Cancer Cells? Antioxidants & Redox Signaling 20(12):1917-1924.
4. Valerio LG Jr. (2007) Mammalian Iron Metabolism. Toxicology Mechanisms and Methods 17(9):497-517.
5. Anderson ER, Shah YM. (2013) Iron Homeostasis in the Liver. Compehensive Physiology 3(1):315-330.
6. Andrews NC. (1999) Disorders of Iron Metabolism. The New England Journal of Medicine 341(26):1986-1995.
7. Octave JN, Schneider YJ, Trouet A, Crichton RR. (1983) Iron uptake and utilization by mammalian cells. I: Cellular uptake of transferrin and iron. Trends in Biochemical Sciences 8(6):217-220.
8. Qian ZM, Tang PL. (1995) Mechanisms of iron uptake by mammalian cells. Biochimica et Biophysica Acta 1269(3):205-214.
9. Hentze MW, Muckenthaler MU, Galy B, Camaschella C. (2010) Two to Tango: Regulation of Mammalian Iron Metabolism. Cell 142(1):24-38.
10. Evstatiev R, Gasche C. (2011) Iron sensing ang signaling. Gut 61(6):933-952.
11. Basilion JP, *et al.* (1994) Overexpression of Iron-

responsive Element Binding Protein and its Analytical Characterization as the RNA-binding form, Devoid of an Iron-Sulfur Cluster. Archives of Biochemistry and Biophysics 311(2):517-522.

12. Gray NK, Hentze MW. (1994) Iron regulatory protein prevents binding of the 43S translation pre-initiation complex to ferritin and eALAS mRNAs. The EMBO Journal 13(6):3882-3891.

13. Salahudeen AA, *et al.* (2009) An E3 Ligase Possessing an Iron-Responsive Hemerythrin Domain Is a Regulator of Iron Homeostasis. Science 326(5953):722-726.

14. Vashisht AA, *et al.* (2009) Control of Iron Homeostasis by an Iron-Regulated Ubiquitin Ligase. Science 36(5953):718-721.

15. Moroishi T, Nishiyama M, Takeda Y, Iwai K, Nakayama KI. (2011) The FBXL5-IRP2 axis is integral to control of iron metabolism *in vivo*. Cell Metabolism 14(3):339-351.

16. Hermand D. (2006) F-box proteins: more than baits for the SCF? Cell Division 1:30. doi: 10.1186/1747-1028-1-30

17. Kipreos ET, Pagano M. (2000) The F-box protein family. Genome Biology 1:reviews3002.1. doi: 10.1186/gb-2000-1-5-reviews3002

18. Jin J, Cardozo T, *et al.* (2004) Systematic analysis and nomenclature of mammalian F-box proteins. Genes & Development 18(21):2573-2580.

19. Skowyra D. *et al.* (1997) F-Box Proteins Are Receptors that Recruit Phosphorylated Substrates to the SCF Ubiquitin-Ligase Complex. Cell 91(2):209-219.

20. Skaar JR, Pagan JK, Pagano M. (2013) Mechanisms and function of substrate recruitment by F-box protein. Nature Reviews Molecular Cell Biology 14:369-381. doi: 10.1038/nrm3582

21. Shu C, *et al.* (2012) The Structural Basis of Iron Sensing by the Human F-box protein FBXL5. Chembiochem 13(6):788-791.

22. Thompson JW, *et al.* (2012) Structural and Molecular Characterization of Iron-sensing Hemerythrin-like Domain within F-box and Leucine-rich Repeat Protein 5 (FBXL5). Journal of Biological Chemistry 287(10):7357-7365.

23. Chollangi S, *et al.* (2012) Hemerythrin-like Domain within F-box and Leucine-rich Repeat Protein 5 (FBXL5) Communicates Cellular Iron and Oxygen Availability by Distinct Mechanisms. Journal of Biological Chemistry 287(28):23710-23717.

24. Wang H, *et al.* (2020) FBXL5 Regulates IRP2 Stability in Iron Homeostasis via an Oxygen-Responsive [2Fe2S] Cluster. Molecular Call 78(1):31-41.e5.

25. Okutani H. (2011) Heme binding controls the function of Iron Regulatory Protein (Unpublished Master's Thesis). Hokkaido University, Sapporo, Japan.

26. ProtParam. (n.d.) Retrieved November 11, 2013, from http://web.expasy.org/protparam/

27. Thiede B, *et al.* (2005) Peptide mass fingerprinting. Methods 35(3):237-247.

28. Ding Q, Xiao, *et al.* (2003) Unmatched peptide mass fingerprints caused by cross-contamination: an updated statistical result. Proteomics 3(7):1313-1317.

29. Joshi V, Shivach T, Yadav N, Rathore AS. (2014) Circular Dichroism Spectroscopy as a Tool for Monitoring Aggregation in Monoclonal Antibody Therapeutics. Analytical Chemistry 86(23):11606-11613.

30. Chen YH, Yang JT. (1971) A New Approach to the Calculation of Secondary Structures of Globular Proteins by Optical Rotatory Dispersion and Circular Dichroism. Biochemical and Biophysical Research Communications 44(6):1285-1291.

31. Wang J, *et al.* (2007) Iron-dependent Degradation of Apo-IRP1 by the Ubiquitin-Proteasome Pathway. Molecular and Cellular Biology 27(7):2423-2430.

32. Kitamura S, *et al.* (2012) The APOBEC3C crystal structure and the interface for HIV-1 Vif binding. Nature Structural and Molecular Biology 19(10):1005-1010.

33. Ishida T, Kinoshita K. (2007) PrDOS: prediction of disordered protein regions from amino acid sequence. Nucleic Acids Research 35(Web server issue):W460-464. doi: 10.1093/nar/gkm363

34. Linding R, *et al.* (2003) Protein Disorder Prediction: Implications for Structural Proteomics. Structure 11(11):1453-1459.

35. Viñas-Castellas R, *et al.* (2013) Nuclear ubiquitination by FBXL5 modulates Snail1 DNA binding and stability. Nucleic Acids Research 42(2):1079-1094.